Quantum Yields of Photoacid Generation in 193-nm Chemically Amplified Resists by Fluorescence Imaging Spectroscopy

Krishanu Ray,* Michael D. Mason, and Robert D. Grober

Department of Applied Physics, Yale University, New Haven, Connecticut 06520-8284

Gerd Pohlers, Carolyne Staford, and James F. Cameron

Microelectronics Materials Research and Development Laboratories, Shipley Company, Marlborough, Massachusetts 01752

Received April 1, 2004. Revised Manuscript Received October 5, 2004

We have made significant improvements in the development of a fast, convenient fluorescence imaging technique for evaluating the acid generation efficiency of photoacids in chemically amplified photoresists. A pH sensitive fluorescent molecule, coumarin 6 (C6), is doped into a 193-nm commercial resist system for imaging. For the 193-nm resist systems studied here, the K_a of C6 lies within the range of acid concentrations that can be photogenerated, making it a suitable probe of the acid generation efficiency of various photoacid generators (PAGs). Resist formulations, each containing a candidate PAG, are doped with C6. The resist is spin coated onto wafers and patterned with 5-μm features, with each feature at a different exposure dose. Each wafer is then spectroscopically imaged with an epi-fluorescence microscope. The spectroscopic content of each feature in the dose ramp is determined and the resulting data are analyzed using a two-level optical titration model. The relative quantum yields of acid generation for several PAGs have been measured multiple times over the span of several months and are shown to be reproducible. Furthermore, we have compared the on-wafer fluorescence imaging technique with two nonindicator based (*C*-parameter and *P*-parameter) methods. Our results demonstrate an excellent agreement among the three techniques.

Introduction

The drive to reduce the size of features printed in photoresist has pushed the lithographic process to increasingly shorter wavelengths. As the exposure wavelength decreases, the photon flux of light sources in modern microlithography tools decreases dramatically resulting in increased processing time. Chemically amplified resists (CARs)[1] are becoming more important throughout the semiconductor industry due to the need for high throughput using these at shorter exposure wavelengths. CARs contain a photoacid generator (PAG) within a polymer-resist. Photolytic decomposition of PAG compounds[2] during exposure generates a strong acid in the resist. This acid acts as a catalyst for many cross-linking reactions between polymer chains. Thus, one incident photon can be responsible for many chemical events. The efficiency of a PAG is quantified by the amount of photoacid created per exposure dose of radiation and depends on its particular properties, such as chemical structure and molecular weight. Understanding the mechanism and efficiency of acid generation is of immense importance for their potential use in the design of more efficient photoinitiators. Because the PAG is an essential component of CARs, evaluation of the quantum yields of photoacid generation of PAGs is an important parameter for resist design. Acid quantification is typically accomplished by spectrophotometric or spectrofluorometric titration of pH indicator dyes.[3−5] The optical titration techniques that are commonly used are destructive and time-consuming because they are performed by dissolution of the exposed resist films, typically with one dose per wafer.

* To whom correspondence should be addressed. E-mail: krishanu.ray@yale.edu.

(1) (a) Macdonald, S. A.; Willson, C. G.; Frechet, J. M. J. *Acc. Chem. Res.* **1994**, *27*, 151. (b) Lamola, A. A.; Szmanda, C. R.; Thackeray, J. W. *Solid State Technol.* **1991**, *34*, 53. (c) Monroe, B. M.; Weed, G. C. *Chem. Rev.* **1993**, *93*, 435. (d) Reichmanis, E.; Houlihan, F. M.; Nalamasu, O.; Neenan, T. X. *Chem. Mater.* **1991**, *3*, 394. (e) Seeger, D. *Solid State Technol.* **1997**, *40*, 115. (f) Ito, H. *Proc. SPIE-Int. Soc. Opt. Eng.* **1999**, *3678*, 2. (g) Pawloski, A. R.; Nealey, P. F. *Chem. Mater.* **2001**, *13*, 4154.

(2) (a) Pappas, S. P. *J. Imaging Technol.* **1985**, *11*, 146. (b) Coenjarts, C.; Garcia, O.; Llauger, L.; Palfreyman, J.; Vinette, A. L.; Scaiano, J. C. *J. Am. Chem. Soc.* **2003**, *125*, 620.

(3) Polster, J.; Lachmann, H. *Spectrometric Titrations*; VCH: New York, 1989.

(4) (a) Buhr, G.; Dammel, R.; Lindley, C. R. *Polym. Mater. Sci. Eng.* **1989**, *61*, 269. (b) Thackeray, J.; Denison, M.; Fedynyshyn, T.; Kang, D.; Sinta, R. *ACS Symp. Ser.* **1995**, *614* (Microelectronics Technology), 110. (c) McKean, D. R.; Schaedeli, U. P.; MacDonald, S. A. *Polym. Mater. Sci. Eng.* **1989**, *60*, 45. (d) McKean, D. R.; Schaedeli, U. P.; MacDonald, S. A. *ACS Symp. Ser.* **1989**, *412* (Polymers in Microlithography), 27. (e) McKean, D. R.; Schaedeli, U. P.; MacDonald, S. A. *J. Polym. Sci., Part A: Polym. Chem.* **1989**, *27*, 3927. (f) Pohlers, G.; Virdee, S.; Scaiano, J. C.; Sinta, R. *Chem Mater*. **1996**, *8*, 2654.

(5) Cameron, J. F.; Fradkin, L.; Moore K.; Pohlers G. *Proc. SPIE (Advances in Resist Technology and Processing XVII)* **2000**, *3999*, 190.

10.1021/cm049448f CCC: $27.50
Published on Web 11/16/2004

Several studies have demonstrated in situ quantification of photoacid in exposed films.[6,7] The advantages of on-wafer techniques are (1) they are nondestructive, (2) they allow measurements to be performed in situ, and (3) they obviate much of the labor-intensive wet chemistry. A potential drawback is that the presence of the indicator can alter the absorbance of the resist at the lithographic wavelength as well as promote PAG decomposition through sensitization during the optical measurement. However, high-sensitivity fluorescence detection permits the use of extremely lower indicator concentrations, thereby minimizing any perturbation of the resist system. In situ studies have typically involved serial measurements (i.e., one acid concentration per measurement event).[8−10]

In earlier publications,[11,12] we have reported the extension of the in situ technique to parallel data acquisition, which is accomplished by spectroscopic imaging of wafers exposed with a dose ramp. The convenience and speed of the parallel scheme is especially relevant in the context of screening many candidate PAGs.[12] Unfortunately, due to relatively high background fluorescence endemic to previous experimental realizations of this technique,[12] a significant correction factor was necessary in the data analysis that turned out to dominate the subsequent error analysis. Furthermore, film and signal heterogeneity over the entire wafer required an additional signal normalization and decreased the achieved reproducibility of the technique. In this paper, we present an improvement of our previously reported parallel in situ acid quantification technique[12] to evaluate the quantum yields of candidate PAGs. The dose array area has been reduced to a 100 $\times$ 100 μm^2 image with individual feature sizes of only 5 μm. This makes it possible to image the entire sample as a single image in an epi-fluorescence microscope, dramatically reducing the influence of background fluorescence and the effect of long-range film heterogeneity. The previous systematic errors reported in evaluating acid generation curves[12] have been eliminated with the present experimental set up.

There already exist two industrially relevant methods of obtaining information about the acid concentration in CARs, neither of which use indicator dyes during film formation. The *C*-parameter method was developed by Szmanda et al.[13] In this method, the photogenerated acid is titrated against increasing amounts of base.

Scheme 1. Protonation Equilibrium of Coumarin 6 (C6)

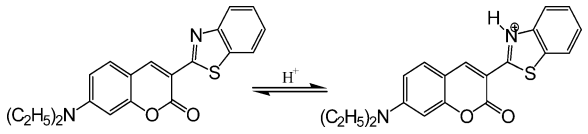

Scheme 2. Chemical Structure of Photoacid Generators

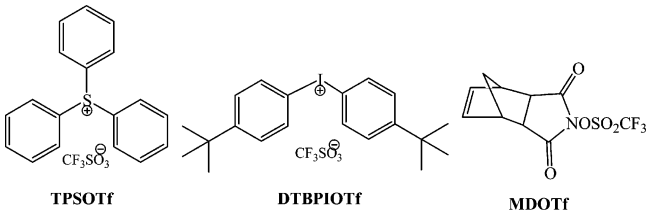

TPSOTf **DTBPIOTf** **MDOTf**

Since the dose to clear (E_0) decreases linearly with the concentration of base, it is possible to infer the amount of acid generated by each exposure and thus ascertain the *C*-parameter. This method does not measure the photoacid directly but rather is an indirect measurement method relying on a lithographic response (E_0) for acid quantification. The principal advantage of this method is that it is efficient and relatively easy to implement requiring only simple E_0 determination for a few resists at various base/PAG ratios. For this reason, this method finds considerable utility in quantifying acid generation for chemically amplified resists under a wide variety of exposure conditions ranging from optical to non-optical exposures: 248-nm, 193-nm, 157-nm, E-beam, EUV, X-ray, and ion projection lithography.[5,13]

The second method was developed by Pohlers et al.[14] and is called the *P*-parameter method. The P-parameter quantifies the photospeed of the sample as if the PAG were the only absorber at the excitation wavelength. This technique introduces a great simplification over other methods in that it does not require samples be specially prepared for the measurement. The *P*-parameter is very useful from the lithographer's point of view, as it expresses the efficiency of a PAG in terms of a photospeed rather than as a quantum yield. Here, we present a comparison of our improved on-wafer fluorescence technique with both the *C*-parameter and *P*-parameter methods for various photoacid generators in 193-nm photoresists.

Experimental Section

Commercially available Coumarin 6 (C6) (Aldrich) was recrystallized from CH_3OH/CH_2Cl_2. The neutral-monocation protonation equilibrium of C6 is shown in Scheme 1. The PAGs triphenylsulfonium triflate (TPSOTf), di[(4-tery-butyl)phenyl]-iodonium triflate (DTBPIOTf), and N-(trifluoromethanesulfonyloxy)-5-norborene-2,3-dicarboximide (MDOTf) were synthesized at Shipley Company Inc. and their structures are shown in Scheme 2. Each of these PAGs generates trifluoromethanesulfonic acid (TFA). The structure of 193-nm positive tone resist obtained from Shipley is shown in Scheme 3.

Three 193-nm resist formulations were prepared, each containing a different PAG (TPSOTf, DTBPIOTf, MDOTf) and doped with 0.05 wt % (vs solid content) C6. The PAG loading

(6) Pohlers, G.; Scaiano, J. C.; Sinta, R. F. *Chem. Mater.* **1997**, *9*, 3222.
(7) Okoroanyanwu, U.; Byers, J.; Cao, T.; Weber, S. E.; Wilson, C. G. *Proc. SPIE-Int. Soc. Opt. Eng.* **1998**, *3333*, 747.
(8) Eckert, A. R.; Moreau, W. M. *Proc. SPIE-Int. Soc. Opt. Eng.* **1997**, *3049*, 879.
(9) Bukofsky, S. J.; Feke, G. D.; Wu, Q.; Grober, R. D.; Dentinger, P. M.; Taylor, J. W. *Appl. Phys. Lett.* **1998**, *73*, 408.
(10) Dentinger, P. M.; Lu, B.; Taylor, J. W.; Bukofsky, S. J.; Feke, G. D.; Hesseman, D.; Grober, R. D. *J. Vac. Sci. Technol.* **1998**, *B16*, 3767.
(11) Feke, G. D.; Hessman, D.; Grober, R. D.; Lu, B.; Taylor, J. W. *J. Vac. Sci. Technol.* **2000**, *B18*, 136.
(12) Feke, G. D.; Grober, R. D.; Pohlers, G.; Moore, K.; Cameroon, J. F. *Anal. Chem.* **2001**, *73*, 3472.
(13) (a) Szmanda, C. R.; Kavanagh, R.; Bohland, J.; Cameron, J.; Trefonas, P.; Blacksmith, R. *Proc. SPIE (Advances in Resist Technology and Processing XVI)* **1999**, *3678*, 857. (b) Szmanda, C. R.; Brainard, R. L.; Mackevich, J.; Awaji, A.; Tanaka, T.; Yamada, Y.; Bohland, J.; Tedesco, S.; Dal'Zotto, B.; Bruenger, W.; Torkler, M.; Fallman, W.; Loeschner, H.; Kaesmaier, R.; Nealey, P. M.; Pawloski, A. R. *J. Vac. Sci. Technol. Ser. B* **1999**, *17*, 3356.
(14) Pohlers, G.; Suzuki, Y.; Chan, N.; Cameron, J. *Proc. SPIE-Int. Soc. Opt. Eng.* **2002**, *4690*, 178.

Scheme 3. Chemical Structure of 193-nm Photoresist

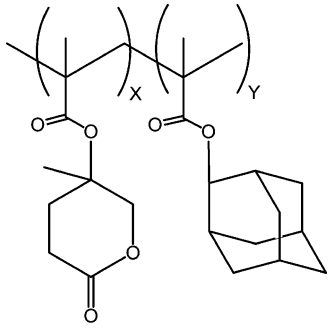

in all formulations was such that the films all exhibited equivalent absorbance at 193 nm. The formulations were spin-coated to a thickness of ~400 nm onto 8-in. bare silicon wafers and received a postapplication bake (PAB) at 120 °C for 60 s. Each wafer was exposed at 193 nm using an ISI microstepper and a mask with a single 5 × 5 μm square. Using a raster scan pattern, a 10 × 10 array of squares was generated with a linear dose ramp from 0.1 to 49.6 mJ/cm^2. The exposure doses for two consecutive squares differ by 0.5 mJ/cm^2. The exposed wafers were placed in separate containers and sealed in plastic bags and kept in dry ice before the measurement in the epi-fluorescence microscope. During the course of the experiments presented here significant airborne base contamination was not observed, which would be manifested as a change in the relative signals in each fluorescence channel.

In general, the absorption and fluorescence spectra of C6 depend on the chemical composition of the surrounding matrix. We have performed absorption and fluorescence spectroscopy of the neutral (C6) and protonated (C6$^+$) forms of the fluorophore in the 193-nm resist. Trifluoromethanesulfonic acid (TFA) was used to protonate the C6 molecule. Spin-coated films were made on quartz substrates for performing the absorption and fluorescence measurement. Absorption spectra were recorded using a Varian CARY 13 spectrophotometer. The absorption spectrum of C6$^+$ shows a large red-shift compared to that of C6 and little overlap exists between the two spectra (Figure 1). Fluorescence spectra were also obtained from the same samples as shown in Figure 1. It is apparent from Figure 1 that the red-shift from C6 to C6$^+$ is so large that the overlap between the two spectra is relatively small.

The apparatus used for acquiring images is based on a Zeiss Axioskop 50 microscope operated in epi-fluorescence mode, a schematic representation of which is shown in Figure 2. Spectroscopic filters were chosen to excite and detect the neutral and protonated C6 population of the dye. Light from a 75-W xenon arc lamp is transmitted through a glass diffuser and an excitation filter, reflected by a long-pass dichroic beam splitter, and imaged onto the sample with a Zeiss infinity corrected microscope objective (air, 10×, 0.3 numerical aperture). The fluorescence is imaged onto a liquid-nitrogen-cooled CCD camera consisting of a 512 × 512 array of 24 × 24 μm pixels (Roper Scientific). The combination of a microscope tube

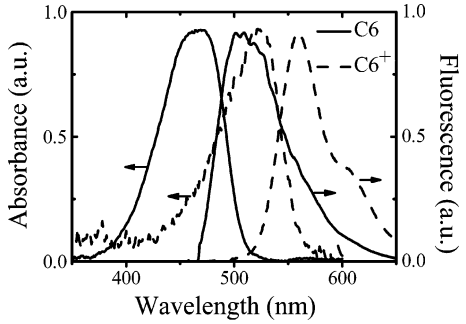

Figure 1. Absorption and fluorescence spectra of C6 and C6$^+$ in 193-nm photoresist.

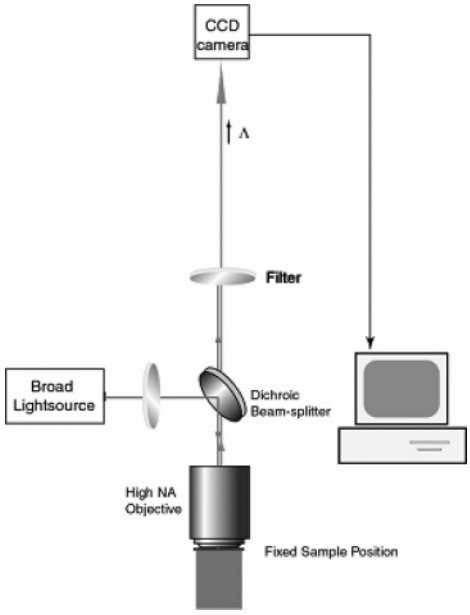

Figure 2. Schematic representation of the experimental setup.

lens and a negative lens provide additional magnification. In general, the fluorescence measurements depend on the filter excitation and collection wavelengths. For detection of C6, a 457.9±5-nm filter was used for excitation, and a 490±20-nm filter was used in series with a 470-nm long-pass filter for collection and suppression of the small amount of scattered excitation light from surface contaminants. Fluorescence spectra (as shown in Figure 1) suggest that C6$^+$ population is very weakly excited by light at 457.9 nm and is very weakly fluorescent between 470 and 510 nm. This choice of filters therefore provides detection of C6 with excellent contrast. For detection of C6$^+$, a 514.5±1.5-nm filter was used for excitation, and a 550-nm long-pass filter was used in series with a 514.5±5-nm notch filter for collection and suppression of the small amount of scattered excitation light from the surface contaminants. C6 does not fluoresce on excitation with 514.5 nm. Images were acquired using an integration time of 30 s. Sample heterogeneity and reproducibility were confirmed by imaging arrays acquired at varying exposed locations on the wafer (data not shown).

Results and Discussion

The photospeed of resists is determined using wafers exposed with a dose ramp pattern, as described in the previous section. The entire dose array (100 μm × 100 μm) has dimensions smaller than the field of view of our imaging system, which allows us to image the entire array in a single acquisition. As the array size is several orders smaller than our previous method,[12] we observed fewer film inhomogeneities across the region of interest, and as a result data analysis is dramatically simplified. Furthermore, the use of a light tight microscope nearly eliminates the contribution of stray background radiation, which plagued our earlier technique, and necessitated the use of relatively large background correction terms ($\beta_{\Lambda 1}$ and $\beta_{\Lambda 2}$).[12]

In the following analysis, we adopt the notation $\Lambda \equiv \{\lambda_{\text{excitation}}, \lambda_{\text{collection}}\}$ to represent filters used for a particular set of measurements. We define $\Lambda_1 \equiv$ {457.9±5 nm, 490±20 nm} and $\Lambda_2 \equiv$ {514.5±5 nm, >550 nm}. Representative Λ_1 and Λ_2 images of the 193 nm-exposed wafers containing TPSOTf are shown in Figure 3. The fluorescence intensity of the features in the Λ_1 image

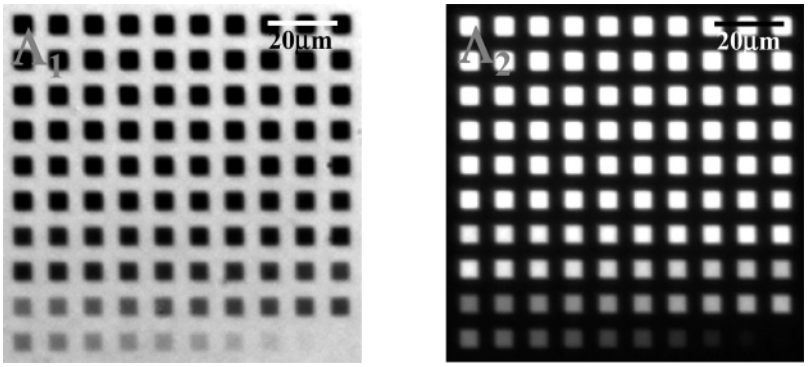

Figure 3. Λ_1 and Λ_2 images of wafers coated with formulations containing TPSOTf and exposed at 193 nm. The dose ramp is exposed in a raster pattern beginning at the lower right and ending at the upper left. The doses are from 0.1 to 49.6 mJ/cm^2 with an increase of each exposure dose in each step by 0.5 mJ/cm^2.

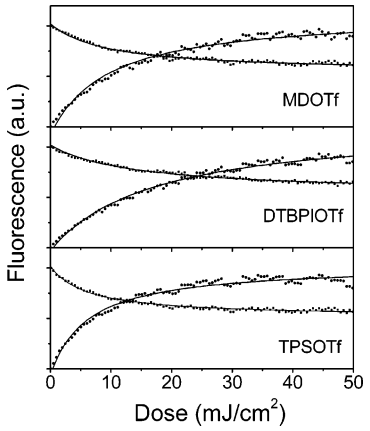

Figure 4. Λ_1 and Λ_2 fluorescence vs dose (at 193 nm) for each of the three PAGs. The lines are fit of eq 3 to the data.

are seen to decrease with increasing exposure dose. This is because the fraction of unprotonated C6 is decreasing. Inversely, the fluorescence intensity in the Λ_2 image increases with increasing exposure dose. The fluorescence intensity from each of the square features in the dose ramp is measured and an intensity vs exposure dose curve is obtained as shown in Figure 4, for three different photoacid generators.

The following optical titration model is used for data analysis. Acid generation curves[12] were found to be well described by the function

$$[H^+] = [H^+]_\infty \frac{E}{(E + E_{1/2})} \tag{1}$$

where $[H^+]$ is the acid concentration for a given exposure dose E, $[H^+]_\infty$ is the acid concentration extrapolated to infinite exposure dose, and $E_{1/2}$ is the exposure at which $[H^+] = [H^+]_\infty/2$. In general, the signal obtained in each detection channel in a two-state optical titration is given by

$$F_\Lambda = F_{C6,\Lambda}\frac{[C6]}{[C6] + [C6^+]} + F_{C6^+,\Lambda}\frac{[C6^+]}{[C6] + [C6^+]} + b_\Lambda \tag{2}$$

where [C6] ([C6$^+$]) is the molar concentration of C6 (C6$^+$) and $F_{C6,\Lambda}$ ($F_{C6^+,\Lambda}$) is the fluorescence measured from an equivalent ensemble with [C6$^+$] ([C6]) equal to zero. The additive background, b_Λ, is related to systematic noise. This background is normalized by the fluorescence intensity at each wavelength (Λ_1, Λ_2) and expressed as: $\beta_{\Lambda_1} \equiv b_{\Lambda_1}/F_{C6,\Lambda_1}$, $\beta_{\Lambda_2} \equiv b_{\Lambda_2}/F_{C6,\Lambda_2}$. In our current epifluorescence microscope setup, we measure β_{Λ_1} and β_{Λ_2} to be 0.009 ± 0.001. This is a dramatic improvement from our previous technique where the values of β_{Λ_1} and β_{Λ_2} were estimated to be 0.05 ± 0.025.

Expressing eq 2 in terms of our two collection wavelengths (Λ_1, Λ_2), and following simplification, we obtain

$$F_{\Lambda_1} = \frac{EP_1 + P_2}{E + P_3};\ F_{\Lambda_2} = \frac{EP_4 + P_5}{E + P_3} \tag{3}$$

where P_1, P_2, P_3, P_4, and P_5 are described in detail in ref 12. Equations 3 are simultaneously fit to the data with P_1, P_2, P_3, P_4, and P_5 as free parameters. The data and fit curves are shown together in Figure 4.

The mixed dissociation constant, K_a, exhibits a linear dependence on [C6] and [C6$^+$], typical of a two level titration. We have previously obtained the value of K_a for C6 [$3.57 \pm 0.16 \times 10^{-2}$ (10^{-3} mol/cm^3)] from in vitro experiments for this system.[12] This value is used in the analysis of the 193-nm exposure data for which $[H^+]_\infty$ and $E_{1/2}$ are unknown (i.e. free parameters). Finally, the values for $[H^+]_\infty$ and $E_{1/2}$ are obtained as

$$[H^+]_\infty = \frac{K_a\left(\frac{P_2}{P_1P_3} - 1\right)}{\left(1 - \left(\frac{\beta_{\Lambda_1}}{1 + \beta_{\Lambda_1}}\right)\frac{P_2}{P_1P_3}\right)}$$

$$E_{1/2} = \frac{P_2}{P_1}\left(\frac{1}{1 - \beta_{\Lambda_1}\left(\frac{P_2}{P_1P_3} - 1\right)}\right) \tag{4}$$

Figure 5 shows acid generation curves for each of the three candidate PAGs. The three curves in each subplot of Figure 5, representing three independent measurements, were taken over a period of three months and demonstrate the reproducibility of our measurement to be of order 10%.

For comparison, we chose TPSOTf as the reference PAG. The relative quantum yield of photoacid generation of each PAG (assuming the films have equal absorbance at 193 nm) is given by $\phi_{gen,rel} \equiv [H^+]/[H^+]_{ref}$. Values of $\phi_{gen,rel}$ for three different PAGs are given in Table 1. We infer that the relative quantum yield is highest for TPSOTf, which would be favored as a

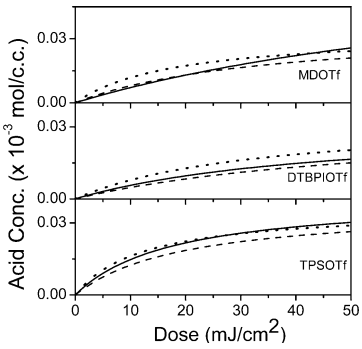

Figure 5. Acid generation curves obtained as a function of dose for three PAGs. Dotted, dashed, and solid lines in each subplot are from the different batches of samples with same resist formulations.

Table 1. Relative Quantum Yields and Acid Generation Parameters for Three PAGs

PAG	$[H^+]_\infty$ (10^{-3} mol/cm^3)	$E_{1/2}$ (mJ/cm^2)	$\Phi_{gen,\,rel}$
TPSOTf	0.036	12.26	1.00
DTBPIOTf	0.034	33.36	0.39
MDOTf	0.033	18.08	0.55

Table 2. Comparison of Acid Generation Parameters for *P*-Parameter, *C*-Parameter, and On-Wafer Fluorescence Method for Three Different PAGs

PAG	*P*-parameter [mJ/cm^2][a]	absolute Φ_{H+} (*C*-parameter)[b]	absolute Φ_{H+} (on-wafer)
TPSOTf	1.10	0.121	0.121
DTBPIOTf	2.86	0.045	0.047
MDOTf	2.47	n/a	0.067

[a] From ref 14. [b] From ref 15.

commercial PAG when compared to the other PAGs used in this study.

For comparison, we measure the quantum yield and the photospeed of the PAGs using two independent methods: the *C*-Parameter and *P*-Parameter, respectively. The *C*-parameter is an indirect method for acid quantification, which estimates the absolute quantum yield (Φ_{H+}) of acid generation.[13] The *P*-parameter method predicts the theoretical photospeed of the formulation if the PAG were the only absorber at the excitation wavelength.[14]

The data for all three methods are compared in Table 2. The relative quantum yields determined with our method were converted into absolute values by assigning TPSOTf an absolute value of $\Phi_{H+} = 0.121$, as previously determined using the *C*-parameter method.[15] We obtain a value of $\Phi_{H+} = 0.047$ for DTBPIOTf, which is in excellent agreement with that obtained by the *C*-parameter method ($\Phi_{H+} = 0.045$).[15]

A comparison with the *P* values is not as straightforward, since *P* is a photospeed rather than efficiency, and it is not expected to correlate in a linear fashion with the quantum yield.[14] In general, a larger *P*-parameter value implies lower relative quantum yield (Φ_{H+}). However, a comparison between *P* and the quantum yields for three PAGs shows that the relative order is the same, i.e., TPSOTf being the fastest/most efficient PAG and DTBPIOTf being the slowest/least efficient PAG.

One advantage of the on-wafer imaging technique as compared to the *P*-parameter method is that it does not depend on the formulation. In addition, all factors that influence the photospeed also impact the absolute value of *P*. This dependency is a direct result of the fact that the actual amount of acid is not determined and the observed photospeed is a convolution of the amount of acid and all the factors affecting the deblocking and dissolution step. It should be pointed out that this dependency of *P* on the processing conditions is shared with the *C*-parameter and the quantum yields extracted from them, whereas our on-wafer optical titration method is independent of both formulation and processing.

Conclusions

We have developed a fast, convenient, and nondestructive fluorescence technique for quantitatively measuring the quantum yields of photoacid generation for 193-nm PAGs. Acid-generation curves and relative quantum yields of PAGs in 193-nm resist systems are obtained with reduced background and a decreased sensitivity to film heterogeneity compared to our previously reported technique.[12] A comparison with two nonindicator-based methods, the well-established *C*-parameter method and the *P*-parameter method, shows good agreement. Our approach is unique because it combines the advantage of in vitro, indicator-based methods with those of on-wafer, E_0-based methods. Specifically, it requires a negligible perturbation of the resist formulation and enables the absolute determination of the acid concentration on the wafer. Additionally, as an in situ method it does not require any wet chemistry and is extremely fast in comparison with the other techniques.

Acknowledgment. This work was supported by the Semiconductor Research Corporation and National Science Foundation under Grant 0211422.

CM049448F

(15) (a) Cameron, J. F.; Moore, K. J.; Chan, N.; Pohlers, G. *Proc. SPIE-Int. Soc. Opt. Eng.* **2001**, *4345*, 106. (b) Cameron, J. F.; Moore, K. J.; Chan, N.; Pohlers, G. *J. Photopolym. Sci. Technol.* **2001**, *14*, 345.